Experimental investigation of fatigue after impact damage growth in CFRP

Biagini, D.; Pascoe, J. A.; Alderliesten, R. C.

DOI
10.1016/j.prostr.2022.12.042

Publication date
2022

Document Version
Final published version

Published in
23rd European Conference on Fracture, ECF 2022

Available online at www.sciencedirect.com

ScienceDirect

Procedia Structural Integrity 42 (2022) 343–350

Structural Integrity Procedia

www.elsevier.com/locate/procedia

23 European Conference on Fracture - ECF23

Experimental investigation of fatigue after impact damage growth in CFRP

D.Biagini[a,*], J.A.Pascoe[a], R.C.Alderliesten[a]

[a] *TUDelft faculty of Aerospace Engineering, Kluyverweg 1, 2629 HS Delft, The Netherlands*

Abstract

Damage propagation in fatigue after impact of CFRP is usually monitored by measuring the external area or simply the one-dimensional width of impact delamination using ultrasound inspection. The present work provides experimental evidence demonstrating that this procedure does not account for all the possible damage propagation taking place in CAI fatigue. In the present work, impact and compression after impact fatigue tests were conducted on CFRP laminates. The impact damage, inspected using through-thickness attenuation ultrasound scan, showed the presence of a non-delaminated cone caused by the out of plane compression during impact. In the following fatigue test, first delamination grew internally inside the non-delaminated cone and, only after, outwards, towards the sides of the specimen. In addition to that, the process of stiffness degradation started before any observable damage growth. This provides experimental confirmation to the necessity to reconsider the current definition of fatigue growth in compression fatigue after impact.

Keywords: Compression after impact; BVID; Delamination; Low velocity impact

1. Introduction

Introducing carbon fiber reinforced polymers (CFRP), allowed to substantially reduce the weight of aircraft primary structures over the past decades. However, knowledge gaps concerning the fatigue strength after impact force designers

* Corresponding author.
E-mail address: D.Biagini-1@tudelft.nl

10.1016/j.prostr.2022.12.042

to introduce large safety factors, preventing them from exploiting the full potential of these materials. Every airplane will eventually face impacts of various severities during its operational life, and for this reason, the impact damage tolerant design of all the exposed surfaces is of paramount importance. Laminates of unidirectional CFRP plies are often preferred to metal alloys due to their enhanced in-plane specific strength but are also known to behave poorly if subjected to out of plane dynamic loading. Low velocity impacts (LVI) in particular, can produce a complex damage envelope, marked on the surface by a small dent, and internally by matrix cracks, delamination and possibly fiber fracture (Ollson (2012)). This scenario, referred to as barely visible impact damage (BVID), is the most concerning, since it is known to significantly reduce the fatigue life of CFRP structures and, due to its low detectability, there is a high chance that airplanes will fly with a non-detected BVID. Of all the possible cyclic loading scenarios, compressive load is regarded as the most critical (Melin et al. (2001)) being capable to trigger unstable failure modes like buckling of sub laminates and fiber kinking.

Several researchers conducted experimental tests of compression fatigue after impact (CFAI) with the goal of characterizing BVID fatigue growth in CFRP. In their early experimental work, Melin et al. (2001) compared buckle areal extension (obtained with DIC) with the delaminated area (monitored using C-Scans) during compression after impact fatigue tests. As the delamination was propagating, the local buckling area was observed to overlap the delamination area and increase at the same rate. This suggested that there was a causal relationship between buckling of sub-laminates and delamination growth during compression cyclic loading. Considering that delamination size determines primarily the buckling load of sub laminates, researchers thought that tracking delamination propagation could be used to assess the fatigue strength degradation. More practically, delamination is easier to detect using ultrasound inspection compared to other damage modes like matrix cracks and fibre breaks.

Because of these two reasons, fatigue of BVID in CFRP has been evaluated using delamination areal growth in previous research. As explained in the review by Davies and Irving (2020) among all the experiments that monitored the delamination growth during CFAI using ultrasound C-scan, inconsistent results can be found. In certain observations (Ogasawara et al. (2013), Tuo et al. (2020), Xu et al. (2017)) there was a transition taking place in which no growth outside of the delamination projected area was observed. After this phase, a single delamination started growing outside of the damage envelope. When this plateau phase in the projected delaminated area was observed, it occupied a major part of fatigue life. In other works instead, a gradual growth of delamination outside the damage envelope was observed from the beginning (Mitrovic et al. (1999), Clark et al. (1987)). This apparent inconsistency in experimental observation, constitutes the biggest knowledge gap in the understanding of fatigue after impact of CFRP. Arguably, it is also because of this challenge that a no-growth philosophy is currently adopted in the certification of CFRP against BVID, as explained in the work of Pascoe (2021).

It can be said that the current definition of fatigue damage growth after impact of CFRP is based on the size of delamination estimated using ultrasound inspection. However, we must consider that ultrasound inspections suffer from well-known limitations.

First, due to shadowing phenomenon, it is not possible to evaluate the growth of a delamination which is positioned in a central depth and surrounded by larger delaminations (Ellison et al. (2020)) (Fig.1.a). A second aspect usually not considered, is the delamination growth below the impact dent. It was reported in literature that BVID shows an area with less or no-delamination exactly below the impact contact point. This is caused by the out of plane compression introduced by the contact during the impact event. Although in this area there is theoretically space for an ulterior growth of delamination in fatigue, as demonstrated in the static CAI tests by Bull et al. (2014), previous studies only focused on the propagation of the external delamination area, mostly because growth in the non-delaminated cone is difficult to evaluate using an echo pulse C-scan due to the reflection caused by the impact dent (Fig.1.b). It is then possible that, while no growth was observed for large part of the fatigue life in previous tests (Ogasawara et al. (2013), Tuo et al. (2020), Xu et al. (2017)) propagation of delamination was actually taking place undetected by the C-scan, in the form of shadowed growth and growth in the non-delaminated cone.

The present work presents experimental evidence demonstrating that the current practice of identifying fatigue damage growth with impact delamination external area/width growth does not cover all the possible damage propagation taking place in CAI fatigue. In particular, it focuses on the phenomenon of growth in the non-delaminated

impact cone. Impact and compression after impact fatigue tests were conducted on CFRP. The impact damage, inspected using through-transmission C-scan, clearly showed the presence of a non-delaminated cone characterized by low attenuation value. Next, a fatigue test was conducted and the delamination propagation was periodically monitored using C-scan. Our results clearly show that first delamination grew in the non-delaminated cone and, only then, growth started outside of initial delamination envelope leading to the final failure of the coupon. This provides experimental confirmations to part of the hypotheses formulated in the previous work of Pascoe (2021). Considering the obtained results, the necessity to reconsider the current definition of fatigue damage growth in compression after impact case is discussed.

Nomenclature

BVID	barely visible impact damage
CAI	compression after impact
CSAI	compression strength after impact
CFAI	compression fatigue after impact
CFRP	carbon fiber reinforced polymers
DIC	digital image correlation
LVI	low velocity impact

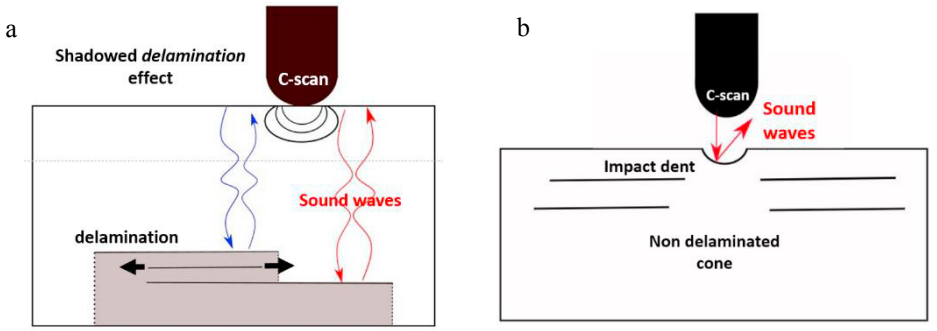

Fig. 1. Limitations of C-scan (a) shadowed delamination growth; (b) impact dent reflection in echo-pulse systems

2. Methodology

2.1. Materials and manufacturing

Toray M30SC Deltapreg DT120-200-36 UD carbon fibre/epoxy prepreg was laid-up in a $[-45, 0, 45, 90]_{4,s}$ laminate for the CAI fatigue tests. Curing was conducted in autoclave following the procedure suggested by the manufacturer. The curing temperature was 120 °C while the maximum pressure was 6 bar. Nominal dimensions of CAI specimens were 150x100x5.15 mm as indicated in the ASTM D7136 standard.

2.2. LVI test

Impact testing was conducted using a drop-weight tower according to ASTM D7136. The test set up is shown in Fig 2a. The support fixture has a cut-out of 125 ± 1 mm in the length direction and 75 ± 1 mm in the width direction. To obtain single impacts, the impact tower was equipped with a catcher triggered by optical sensors. A hemi-spherical impactor with a diameter of 16 mm and a mass of 4.8 kg was used. A target impact energy of 34 J was used in all the impacts. This condition can be classified as low velocity impact (LVI) and produced a dent depth < 0.3 mm (BVID). After the impact, the size of delamination was checked using ultrasound inspection.

2.3. CFAI test

To estimate the CAI static strength, three specimens were tested following ASTM D7137 standard for static CAI tests. Next, since there is no standard for fatigue CAI, testing was conducted using the same setup as for the static CAI tests (Fig.2.b). Two specimens were loaded in compression-compression under force control. The maximum compressive load was 65% and 85% of static CAI failure load with R = 10 and frequency 3 Hz, to avoid heat related phenomena. The crosshead displacement and the applied force were recorded using a 100 kN load-cell on an MTS hydraulic testing machine.

Digital Image Correlation (DIC) was used on the impacted side of the specimens. Due to the high frequency of the fatigue test, it is difficult to obtain steady pictures for DIC analysis. For this reason, to properly capture the deformed shape of the specimen, the test was stopped periodically and a ramp was applied to reach the maximum compressive stress of the fatigue cycle. Then the displacement was kept constant for 1 second in order to take steady picture of the deformed shape. DIC pictures were acquired after 10 and 100 cycles. After that DIC pictures were taken every 1000 cycles until failure was reached.

The test was periodically stopped to allow the inspection of the coupon using ultrasound scan in the water tank located close to the test location (Figure 2c). The procedure of removing, scanning and repositioning the specimens took on average 10 minutes. The ultrasound scan inspection was performed after 10, 100, 1000 cycles. After that the ultrasound inspection was performed periodically every 10’000 cycles until failure was reached.

2.4. DIC

To capture the displacement and strain contour map during the test, a three-dimensional DIC system was used. The system consisted of two 9 MP “Point Grey” cameras with ‘Tamron’ 25 mm lenses (Fig.2.b). The speckle pattern images were captured by ViC-Gauge 3D software, afterwards the images were processed using ‘ViC-3D 8’ software.

2.5. Ultrasound inspection

To evaluate delamination size, through thickness attenuation scan system immersed in a water tank was used (Fig. 2.c). A probe of 8 MHz was used to emit ultrasound towards the receiver placed at 100 mm distance. Scanning speed was set to 100 mm/s and a definition of 1 mm was achieved. The authors decided to perform the analysis using through thickness attenuation system in order to avoid the reflection effects form the top surface of the specimen in the dent region (Fig.1.b) and be able to capture delamination growth below the impact dent area.

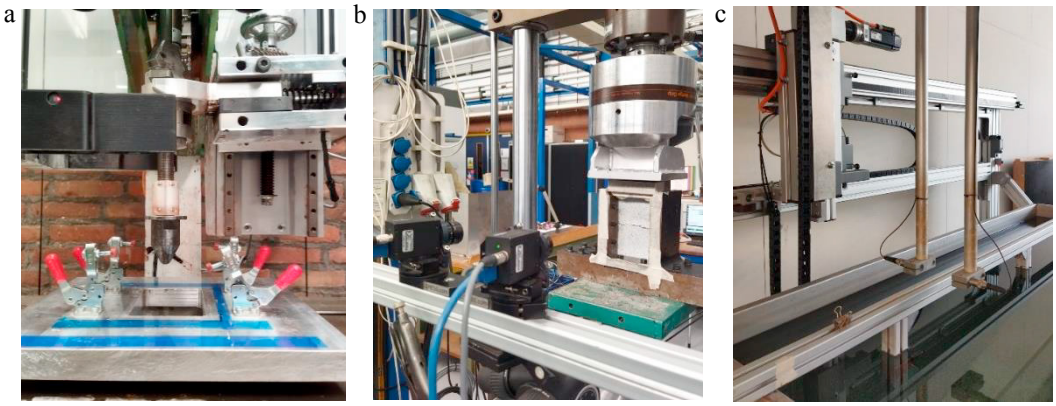

Fig. 2. (a) LVI test setup; (b) CAI test setup: (c) Attenuation scan water tank

3. Results and discussion

3.1. LVI test

Impact tests resulted in BVID (impact dent < 0.3 mm) comprising multiple delaminations at different interfaces as documented in previous experimental works (Bull et al. (2014), Ellison et al. (2020)). From Fig.5, it's evident that a non-delaminated area can be detected in the impact location. The presence of this feature was observed by other authors in the literature both in LVI (Bull et al. (2014), and quasi static indentation (Abisset et al. (2016)) and can be attributed to the out of plane compression originating in the contact region between the impactor and the composite plate.

3.2. CAI Static test

The three CAI static tests showed a constant stiffness until final failure. In all tests, the global buckling was successfully prevented by the lateral guides and local buckling happening in the area of impact was observed using the DIC system. In all three specimens final failure occurred from the impact location towards the lateral edges, which is acceptable according the ASTM D7137 standard. The average failure load was 101 kN.

3.3. CAI fatigue test

Two fatigue tests were conducted on the impacted specimens (section 2.3):

- test-1 *long life fatigue* (65% CSAI) failed at 180'000 cycles.
- test-2 *short life fatigue* (85% CSAI) failed at 2'500 cycles.

To a visual examination, in both tests the failure mode appears to be similar to the one observed in static CAI tests, with a transverse fracture starting at the impact location and propagating towards the lateral edges (Fig.4). The local failure modes observed were delamination and fibre kinking.

In Fig.3, the three components of strain derived using DIC are showed in both tests at 10% and at 90% of fatigue life. In both tests, local buckling of sub-laminates in the area of impact delamination was observed. In the *long-life* test, a more fragmented buckling shape was observed, compared to *short-life* test. This could be caused by local fiber damage observed after impact on the surface of the *long-life* specimen. It must be also considered that, due to the different initial impact damage delamination envelopes, it's hard to obtain the same sublaminate buckling in different tests. Although the work of Xu et al. (2017) observed a sublaminate buckling mode change happening during fatigue in the same type of test, in the present work the DIC analysis didn't show qualitative changes in the strain field suggesting that the sub laminate buckling mode didn't change.

The stiffness was estimated from the loading ramps periodically applied to the specimen to acquire DIC pictures (section 2.3). The stiffness degradation (Fig.6) showed different behaviours in *short-life* fatigue and *long-life* fatigue tests. In *short-life* fatigue test, no significant degradation was recorded before failure. In the *long-life* fatigue test instead, a stiffness degradation was observed. Interestingly, the stiffness degradation was not gradual but assumed the form of drops followed by steady phases with constant stiffness. Particularly interesting is the fact that an abrupt drop in stiffness was recorded at 60'000 cycles followed by a long phase where no degradation was observable.

Periodic ultrasound scan was performed at interrupted fatigue test (Fig.6). In *short-life* fatigue, three scans were performed after 10, 100 and 1000 cycles. In the scans almost no delamination growth was observed and the specimen reached failure at 2500 cycles. In *long-life* fatigue instead, a total of 21 scans were performed following the intervals explained in section 2.4. For large part of the fatigue life no apparent growth was observed. After 140'000 cycles, delamination growth in the initial non-delaminated cone was observable. Only after that, a large delamination growth started in the transverse direction until reaching final failure. As previously explained, the short-life fatigue test showed only little growth. However in this case, due to the short duration of the test and the adopted inspection intervals, the last scan was performed at less than 40% of total fatigue life. For this reason the authors cannot exclude that adopting a shorter inspection interval, a delamination propagation similar to the *long-life* fatigue could be seen in the *short-life* fatigue.

Combining the information from DIC, stiffness measurements and ultrasound scan, two major points emerge:

- The growth in the non-delaminated cone was successfully observed using the ultrasound, but it's *not* sufficient to explain all fatigue damage propagation. When the first stiffness drop was registered in the *long-life* fatigue test, no growth was observed yet inside or outside the delaminated cone. This suggests that other mechanisms could be the cause for this drop of stiffness and that other inspection techniques should be used to investigate this aspect, like acoustic emission.
- The work of Melin et al. (2001) suggested that delamination growth inside the non-delaminated cone could trigger sub-laminate buckling mode change. In the experimental work by Xu et al. (2017) a change in buckling mode prior to the onset of a final growth was observed. However in the present work the buckling mode didn't show changes in correspondence of the growth in the undamaged cone as shown in the strain plots before and after growth in the non-delaminated cone (Fig.3).

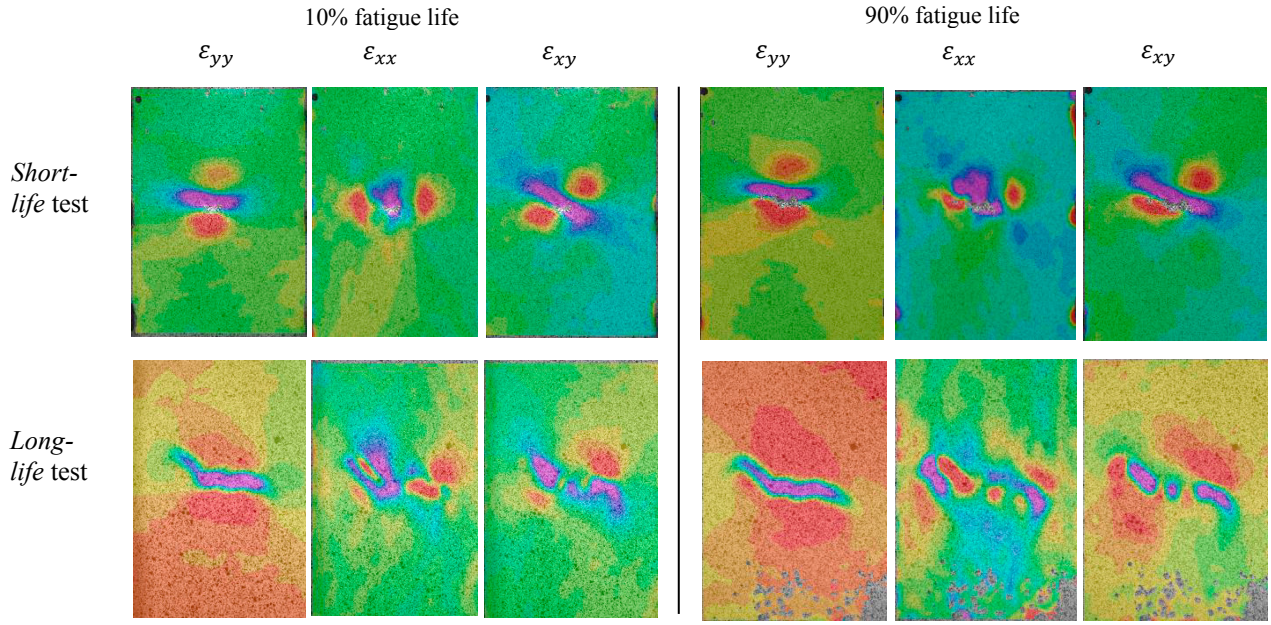

Fig.3. DIC analysis to derive ε_{yy}, ε_{xx}, ε_{xy} strain components in short life and long life fatigue tests at beginning and end of the test

Fig. 4. Failed fatigue specimen showing the presence of delamination and kinking in transverse direction

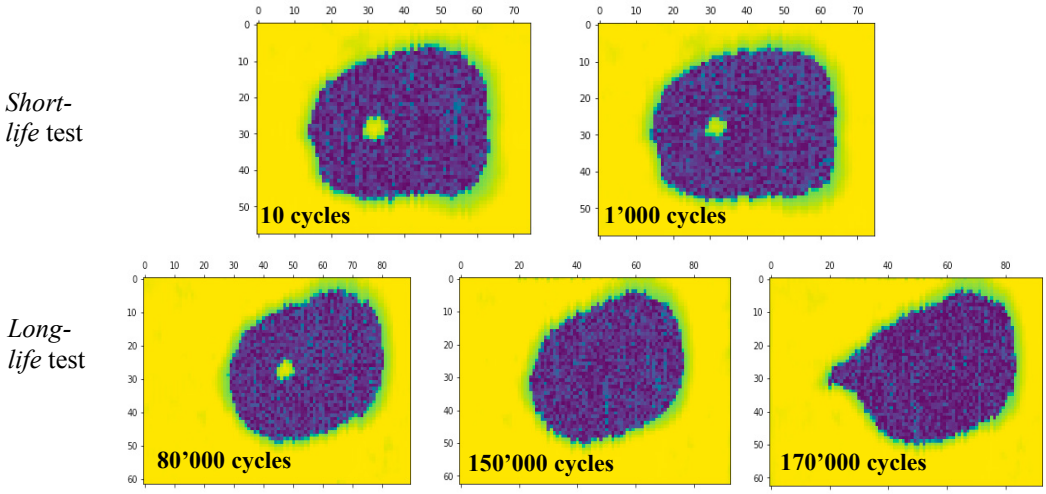

Fig.5. Ultrasound inspection results for *short-life* and *long-life* fatigue test

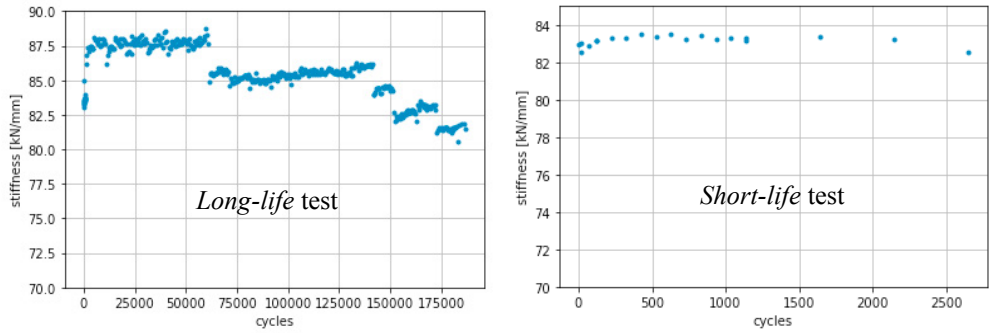

Fig.6. Stiffness degradation in *long-life* and *short-life* fatigue test

4. Conclusions

A series of fatigue after impact tests was conducted to investigate the delamination growth after impact in CFRP. After preliminary static CAI tests, two fatigue tests were conducted: *short-life* fatigue (85% CSAI) and *long-life* fatigue (65% CSAI). From the monitoring of damage propagation, a series of considerations can be made:

- The stiffness degradation in long-life test showed a discontinuous step-type decrease with sudden drops followed by long stable phases.
- The delamination propagation monitored with ultrasound scan showed that first delamination grew in the central impact area below the dent, and only after a transverse growth took place towards the lateral edges.
- Opposite to the work of Xu et al. (2017) no buckling mode change was observed in fatigue. In particular the buckling mode didn't change in correspondence of the growth in the non-delaminated cone.
- Stiffness degradation in the long-life test shows that damage propagation is happening non detected by the ultrasound scan at early stages of fatigue life (60'000 cycles) even before the onset of growth in the non-delaminated cone.

Traditionally damage propagation in fatigue after impact has been monitored using external area or simply width of delamination. The present work clearly shows that this definition can be improved by including delamination growth internal to the damage envelope (in particular in the impact cone). In addition to that, the stiffness drop recorded at 60'000 cycles suggests that additional growth mechanisms could be happening that were not detected with the present

study. Therefore, the investigation presented in this paper could be improved by monitoring acoustic emission during this early phase of fatigue after impact, a possibility that will be explored by the authors in future work.

References

E. Abisset, F. Daghia, X. C. Sun, M. R. Wisnom, and S. R. Hallett, "Interaction of inter- and intralaminar damage in scaled quasi-static indentation tests: Part 1 - Experiments," Composite Structures, vol. 136, pp. 712–726, 2016, doi: 10.1016/j.compstruct.2015.09.061.

D. J. Bull, S. M. Spearing, and I. Sinclair, "Observations of damage development from compression-after-impact experiments using ex situ micro-focus computed tomography," Composites Science and Technology, vol. 97, pp. 106–114, 2014, doi: 10.1016/j.compscitech.2014.04.008.

G. Clark and T. J. van Blaricum, "Load spectrum modification effects on fatigue of impact-damaged carbon fibre composite coupons," Composites, vol. 18, no. 3, pp. 243–251, 1987, doi: 10.1016/0010-4361(87)90414-9.

G. Davies and P. Irving, Impact, post-impact strength, and post-impact fatigue behavior of polymer composites. Elsevier Ltd, 2020. doi: 10.1016/b978-0-08-102679-3.00011-3.

A. Ellison and H. Kim, "Shadowed delamination area estimation in ultrasonic C-scans of impacted composites validated by X-ray CT," 2020, doi: 10.1177/0021998319865311.

L. G. Melin and J. Schön, "Buckling behaviour and delamination growth in impacted composite specimens under fatigue load: An experimental study," Composites Science and Technology, vol. 61, no. 13, pp. 1841–1852, 2001, doi: 10.1016/S0266-3538(01)00085-9.

M. Mitrovic, H. T. Hahn, G. P. Carman, and P. Shyprykevich, "Effect of loading parameters on the fatigue behavior of impact damaged composite laminates," Composites Science and Technology, vol. 59, no. 14, pp. 2059–2078, 1999, doi: 10.1016/s0266-3538(99)00061-5.

T. Ogasawara, S. Sugimoto, H. Katoh, and T. Ishikawa, "Fatigue behavior and lifetime distribution of impact-damaged carbon fiber/toughened epoxy composites under compressive loading," Advanced Composite Materials, vol. 22, no. 2, pp. 65–78, 2013, doi: 10.1080/09243046.2013.768324.

R. Olsson, Low- and medium-velocity impact as a cause of failure in polymer matrix composites. Woodhead Publishing Limited, 2012. doi: 10.1533/9780857095329.1.53.

J. A. Pascoe, "Slow-growth damage tolerance for fatigue after impact in FRP composites: Why current research won't get us there," Theoretical and Applied Fracture Mechanics, vol. 116, Dec. 2021, doi: 10.1016/j.tafmec.2021.103127.

H. Tuo, T. Wu, Z. Lu, and X. Ma, "Evaluation of damage evolution of impacted composite laminates under fatigue loadings by infrared thermography and ultrasonic methods," Polymer Testing, vol. 93, Jan. 2021, doi: 10.1016/j.polymertesting.2020.106869.

F. Xu, W. Liu, and P. E. Irving, "Fatigue life and failure of impact-damaged carbon fibre composites under compressive cyclic loads," ICCM International Conferences on Composite Materials, vol. 2017-Augus, no. August, pp. 20–25, 2017.